


Melanie Werner*
Mathias Ehrenwirth
Sebastian Muschik
Christoph Trinkl
Tobias Schrag

Operational Experiences with a Temperature-Variable District Heating Network for a Rural Community

The potential of utilizing temperature-variable district heating systems in rural areas was investigated. A local district heating system in Germany and the related project NATAR are briefly described; measurement data is evaluated. Operational experiences with a seasonal temperature reduction and consequent advantages for different heat generation systems and heat storages are discussed. The analysis of measurement data reveals a high optimization potential for solar thermal systems in case of an integration both into a low- and a high-temperature storage. Furthermore, a combined heat-and-power plant in combination with a CO₂ heat pump promises sector-coupling potential and high electricity self-consumption.

 This is an open access article under the terms of the Creative Commons Attribution-NonCommercial-NoDerivs License, which permits use and distribution in any medium, provided the original work is properly cited, the use is non-commercial and no modifications or adaptations are made.

Keywords: District heating network, Low temperature, Sector coupling

Received: April 21, 2021; *revised:* May 31, 2021; *accepted:* September 02, 2021

DOI: 10.1002/ceat.202100114

1 Background

With its “Green Deal”, the European Union (EU) set up a plan to tackle climate change, reduce environmental degradation and finally become the first green continent until 2050 [1]. To meet this objectives, it is necessary to increase the share of renewable energies (RE) in all sectors. Industry, services, households, and transportation rank amongst the main energy consumers in the EU [2]. In 2019, 19.7 % of the gross final energy consumption was covered by RE. While the share of RE in the electricity sector has increased considerably (+13.4 %), the heating-and-cooling sector shows a significantly lower increase over the past 10 years (+5.3 %) [3].

The situation in Germany is comparable to the development on the European level, especially concerning the different increases in the shares of RE in the heat and electricity sectors. With a share of RE in the final energy consumption of 17.4 %, Germany occupies the 16th place in the EU [3]. However, an increasing share of RE within the German electricity grid demands proper management and technological solutions to compensate for the fluctuating nature of RE and thus to ensure a stable energy supply. To cope with this situation in the near future, “sector coupling” (i.e. combining the heating, cooling, and mobility sectors) and flexible consumers are potential solutions to meet this challenge.

To manage the changes and challenges of sector coupling, so-called Smart Energy Systems (SES) are proposed [4], which provide the possibility of balancing the fluctuations caused by RE in the electricity grids. By combining the electricity, heating, and gas grids, flexibility is generated to achieve the optimum with respect to the overall energy system. Smart Thermal Grids, or fourth-generation district heating networks (DHN), are part of the SES. Lund et al. [5] describe them as a system with low-

temperature water as a heat transfer fluid. An average temperature between 30 and 60 °C within the grid enables the integration of low-temperature RE. Due to the low temperature, heat losses are reduced compared to third-generation networks, which are typically operated at a temperature level of up to 100 °C [5]. The best possible solution for each energy concept depends on the individual heat requirements of connected consumers [6, 7]. Existing buildings typically require a higher flow temperature compared to new buildings. Therefore, the reduction of the supply temperatures in a heating grid is limited in such cases.

To reduce losses in grids supplying also existing buildings, lowering the supply temperature seasonally provides a promising option. In addition to decreasing transportation losses, this approach improves the efficiency of integrated RE (e.g., solar thermal energy) [8]. As the space heating demand in Germany is low or non-existent during summer, the grid losses might decrease significantly, allowing for a temperature-reduction of the DHN during this period. To provide the necessary supply temperature for domestic hot-water preparation, decentralized heat pumps together with appropriate control strategies allow for a seasonal reduction of the flow temperature and may therefore positively contribute to optimizing DHN.

The decreasing heat connection density over the last years and optimization of DHN to so-called fourth- and fifth-generation DHN (see Buffa et al. [9]) are the subject of ongoing

Melanie Werner, Mathias Ehrenwirth, Sebastian Muschik, Dr. Christoph Trinkl, Prof. Dr.-Ing. Tobias Schrag
melanie.werner@thi.de
Technische Hochschule Ingolstadt, Institute of New Energy Systems,
Esplanade 10, 85049 Ingolstadt, Germany.

research [10–12]. Fifth-generation DHN (also called ultra-low-temperature DHN with less than 30 °C) utilize multiple decentral heat pumps to meet the temperature requirements and can therefore be linked with the electricity sector [13, 14]. Further research regarding fourth- and fifth-generation DHN (and their comparison) was done by Ommen et al. [14], Lund et al. [15], and Yang and Svendsen [16]. In addition, within the collaborative research projects of the International Energy Agency (IEA EBC Annex 84 and IEA DHC Annex TS3), innovative DHN are currently further investigated. However, a temperature-variable DHN could not be found in the literature. A temperature-variable DHN means that it works seasonally, depending on the ambient temperature, as a third- as well as a fourth- or fifth-generation DHN.

Against this background, a temperature-variable DHN was realized in Dollnstein (Germany) and analyzed within a research project. Amongst others, one aim of the project NATAR (2017–2020) was to monitor the DHN with variable temperatures at Dollnstein, to evaluate the advantages and disadvantages of the particular operation characteristic (i.e., switching between the cold and hot modes) and to identify optimization potentials. In a second step, further possibilities to enhance sector coupling were investigated. This research article focuses on the evaluation of measurement data, which are subsequently presented and discussed, and the transferability to similar projects.

2 The Temperature-Variable District Heating Grid in the Rural Community of Dollnstein

In Dollnstein, a rural community located in South Germany, an innovative district heating system following the aforementioned approach of a seasonally variable DHN flow temperature was constructed. It is amongst the first heating systems with variable temperatures and, since 2015, nearly 25 consumers have been connected. The heating network consists of three main hydraulic circuits supplying new and already existing, domestic and commercial/non-domestic buildings (e.g., gym, school). The variety of building types (e.g., a church built in the 18th century, a school, and a city hall) requires high supply temperatures (> 60 °C) in combination with a high heat demand, especially during winter. However, the lower heat demand during German summers (solely hot water demand) allows for improving the energy efficiency and the economic viability by reducing the temperature of the DHN, therefore minimizing its heat losses.

In order to generate heat to supply the DHN, multiple options are available in the central district heating station (DHS; Fig. 1): a CO₂ groundwater heat pump (nominal capacity 440 kW_{th}), a liquid gas-fired combined heat-and-power (CHP) plant (nominal capacity 235 kW_{th}), and a liquid gas-fired backup boiler (nominal capacity 300 kW_{th}). The electricity

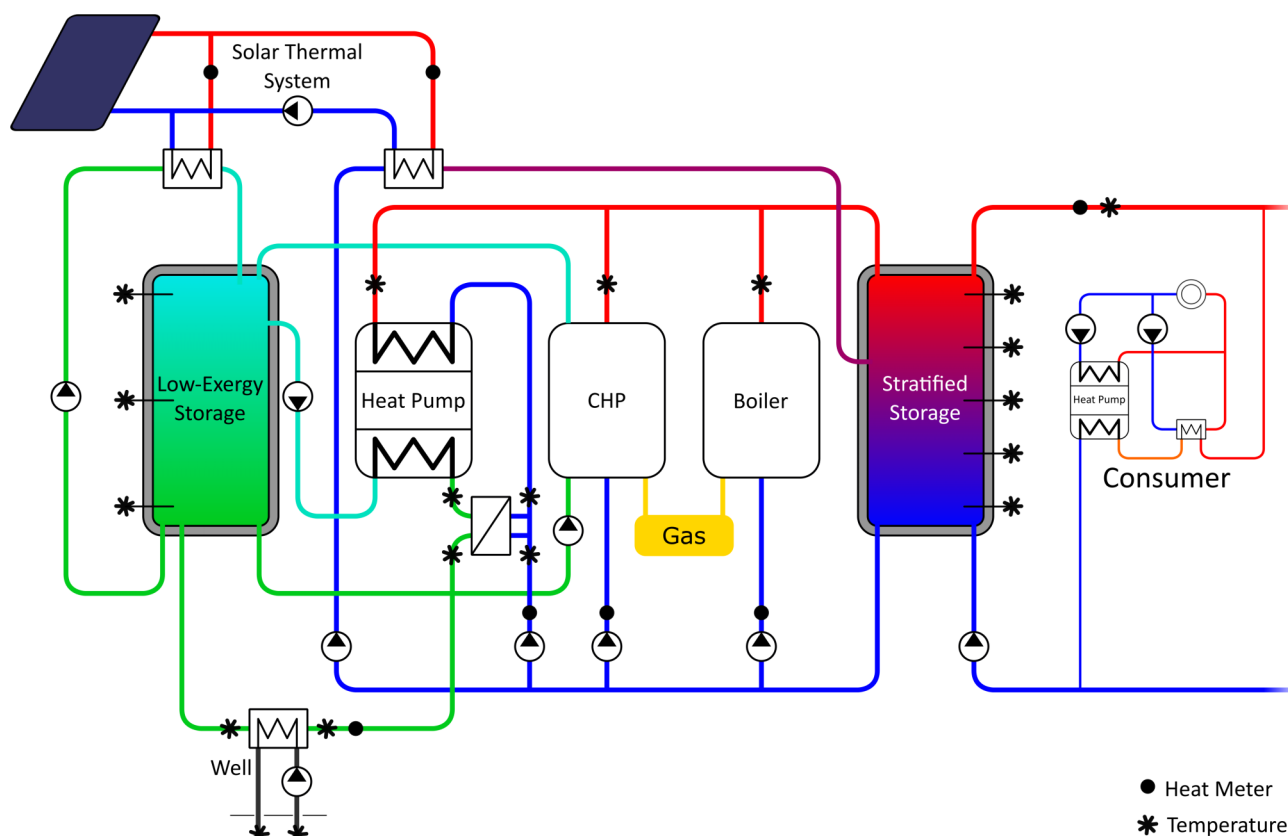


Figure 1. Schematic illustration of the central district heating station in the DHN with selected measurement sensors (adapted to [17]).

generated by the CHP plant is consumed by the central heat pump. Furthermore, 100.4 m² of solar thermal collectors contribute to the heat supply of the system. For the system integration of the four heat generation systems, a low-exergy and a stratified storage are implemented in the central DHS.

The low-exergy storage with a volume of 15 m³ serves – in combination with a groundwater well – as a low-temperature source for the heat pump and can be charged by using the condensing heat of the CHP and the solar thermal collectors. The stratified storage can be supplied by all heating devices, including the solar thermal system, which can therefore charge both the stratified and the low-exergy storage depending on the temperature of the heat transfer fluid. During the winter period (November – May), the DHN usually operates at a supply temperature level of 75 °C to meet the necessary heat demand and operational requirements of the decentral consumers, amounting up to 8 MWh per day. During the summer period (May – November), the flow temperature is lowered to about 40 °C and the central heat pump and the CHP plant are out of operation. Further control algorithms are described in Ramm et al. [17].

Furthermore, pre-insulated duo-pipelines with a total length of 1800 m ensure heat transportation from the central DHS to the consumers. To meet the consumers' heat demand during summer, a buffer storage and decentralized heat pumps are installed at each building. As the consumers widely differ regarding their annual heat demand (non-residential and residential), a variety of buffer storages (500–2000 m³) and heat pumps (1.9–3.1 kW_{el}) are implemented in the decentral substations.

3 Measurement Equipment and Evaluation of Measurement Data

To evaluate the DHN, the Dollnstein system was equipped with extensive measurement equipment, especially the central DHS (Fig. 1). However, as some areas were not time resolved or not recorded at all, retrofitting of the measurement technology was necessary. The recording of the measurement data is event based (i.e., values will only be tracked in case of a change).

The DHN in Dollnstein was planned assuming an annual heat generation of 1.38 GWh to meet the heating demand of 40 private households and several public buildings. In Tab. 1, annual values for the heat production of the central DHS for supplying the DHN are given.

As not every consumer was connected to the DHN in 2018, the annual heat production has continuously increased over the years. In 2020, the measured heat generation of 1.24 GWh was 140 MWh lower than the planned value as there are still consumers with an existing heating system (e.g. oil-fired boilers) working in parallel to the DHN.

Table 1. Annual heat production of the central DHS in Dollnstein.

Year	Heat production [GWh]
2018	1.09
2019	1.17
2020	1.24

As described in Sect. 2, different heating devices were installed in the central DHS. Due to compressor damage of the central heat pump between May and November 2020, further evaluation was performed with values prior to this event. To meet the heat demand, there are four different primary sources of energy, which were directly used for the heating grid or for further heat generation: liquid gas, electric energy, energy from groundwater, and solar energy. In January 2020 (Fig. 2a), the predominant energy source was liquid gas. In contrast, in July 2019 (Fig. 2b), liquid gas amounted to only 5 %. This can be attributed to a high contribution of solar thermal energy during the summer (e.g., 48 % in July 2019). However, nearly the same amount (40 %) is required in the form of electricity from the external electricity grid for the decentral heat pumps and as auxiliary energy to run the whole DHN. A photovoltaic system with 191 kW_p has already been installed next to Dollnstein. However, this power plant is not directly coupled with the Dollnstein system at the moment. Therefore, this electricity cannot yet be used by the DHS itself but must be fed into the external grid.

3.1 Seasonal Temperature Reduction

One of the innovative elements of the DHN in Dollnstein was to lower the supply temperature seasonally to minimize grid heat losses. In 2020, the flow temperature was lowered from May 21 to October 20, with an average value from ~74 °C during the winter period to ~45 °C during the summer period

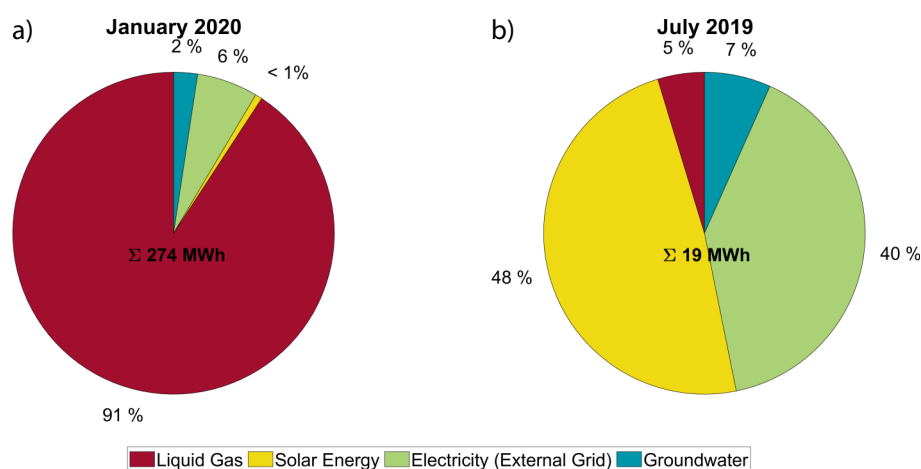


Figure 2. Energy sources for the whole system in the DHN Dollnstein: (a) January 2020, (b) July 2019.

(Fig. 3). As a result, the return temperature is 27 °C, on average, during the summer period and 48 °C during the winter period.

Reducing the flow temperature led to a reduction of the heat losses of the DHN in Dollnstein during the summer months. To determine the heat losses (Q_{loss}), the difference between the energy distributed to the customers ($Q_{\text{DHN}} + P_{\text{el}}$) and the heat fed into the decentralized storage facilities of each consumer ($Q_{\text{Cons.}}$) was derived. In this context, the energy distributed to the customers consists of the supplied heat by the central heat station (Q_{DHN}) as well as the electricity demand of the decentralized heat pumps (P_{el}) (Fig. 4). Here, it has to be noted that the measurement data of one consumer (post office) is not available and was therefore not considered for the subsequent evaluation.

In 2018, the overall heat losses of the DHS in Dollnstein amounted to 279 MWh. Considering an overall amount of 1162 MWh delivered to the DHS, this yields relative heat losses of 24 %. However, a further analysis shows that 88 % of the total heat losses for the entire year occur within the five winter months from November until March. To classify those heat losses, the measurement data is compared to the target values published by Pex [18] (Fig. 5).

In the presentation of Pex [18], 377 DHN with a minimum pipe length of 200 m were investigated. To ensure economical operation, it is recommended that heat losses should be less than 10 % of the total heat supply, with a minimum connection density of $1.5 \text{ MWh m}^{-1} \text{ a}^{-1}$. The DHN in Dollnstein does not achieve these target values. However, with a connection density of $0.5 \text{ MWh m}^{-1} \text{ a}^{-1}$, it matches the regression function made based on all investigated DHN from Pex [18] (Fig. 5).

The real heat losses of the DHN in Dollnstein are expected to be lower than 24 %, since the data of the post office with a connected load of 60 kW was not available for the measurement evaluation. To estimate the heat losses of the post office, the

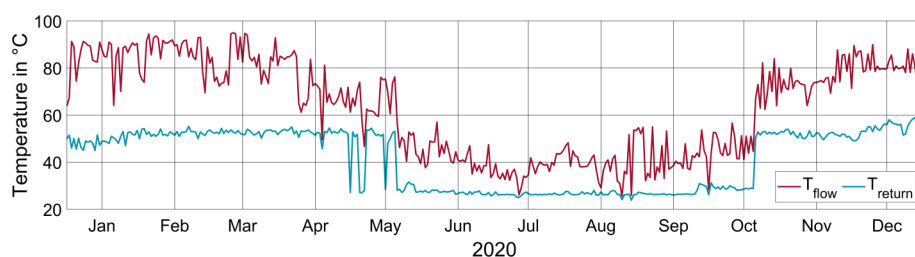


Figure 3. Grid temperatures of the DHN Dollnstein in 2020 with flow (T_{flow}) and return (T_{return}) temperature.

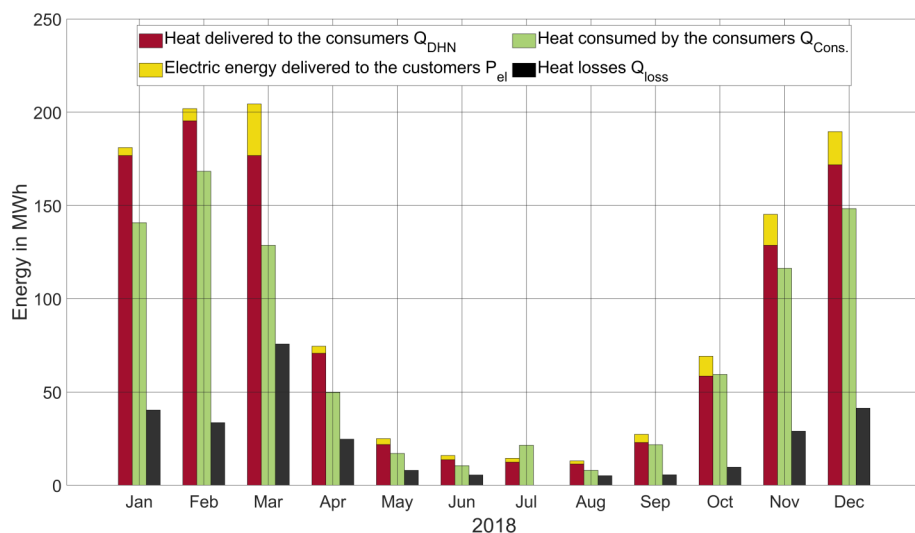


Figure 4. Monthly energy balance (in MWh) of the DHN Dollnstein at the consumers' side to determine heat losses.

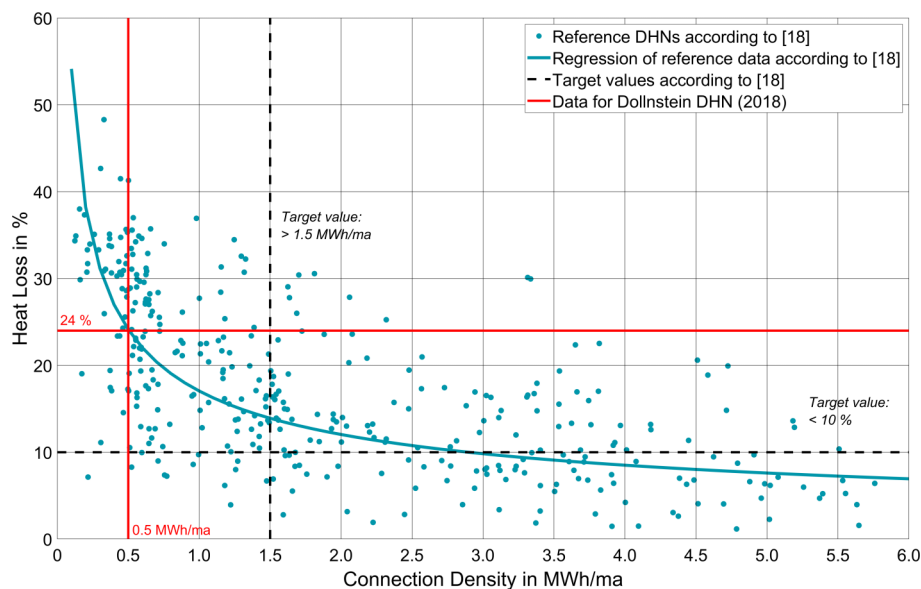


Figure 5. Heat losses and connection density of the DHN in Dollnstein in 2018, compared to reference values adapted to [18].

heat demand for another public building (Rathaus (town hall), 100 kW) was proportionally evaluated. By considering an estimated heat demand of the post office of 55 MWh (4.4 % of the

total heat demand), the heat losses could be reduced to 19 % with a connection density of $0.53 \text{ MWh m}^{-1} \text{ a}^{-1}$.

It can be concluded that seasonally lowering the temperature of the DHN could not reduce the annual heat losses. This can be attributed to the fact that there are currently only 25 consumers (expected: 40). Due to further decentral heat generation systems, the planned heat requirement is higher than the real heat demand. Therefore, the very low heat demand density of the system leads to high losses in general. However, an analysis of the summer shows that the lowered temperatures during summer compensate the losses, which would otherwise be even higher.

3.2 Integration of Solar Thermal Collectors

As mentioned in Sect. 2, 100.4 m^2 of solar thermal collectors are integrated into the DHN in Dollnstein. To increase the share of RE within the temperature-variable DHN, the solar thermal system is explained in detail subsequently. It is a central solar thermal system that supplies the low-exergy storage as well as the stratified storage and is installed on the roof of the central DHS. If the low-exergy storage is fully charged, i.e., the temperature is higher than 20.2°C at the top of the storage, the heat is fed into the stratified storage. Tab. 2 shows the annual solar heat production from 2018 until 2020 and the utilization of the storages. For this period, the collectors delivered more energy to the stratified storage than to the low-exergy storage. This can be attributed to the fact that the solar thermal system is the main heat producer within the DHN during summer. However, it increased significantly due to the breakdown of the central heat pump over five months in 2020 and led to a share of 77.5 % of thermal energy supplied to the stratified storage. As the low-exergy storage serves as a heat source

Table 2. Annual heat production of the solar thermal system and the shares of heat supply fed into each storage.

Year	Total solar heat production [MWh]	To stratified storage [%]	To low-exergy storage [%]
2018	79.9	58.4	41.6
2019	69.7	60.4	39.6
2020	73.8	77.5	22.5

for the central heat pump, the solar thermal system only supplied the stratified storage during the breakdown.

Analyses of measurement data further indicate that heat was fed into the stratified storage even on sunny winter days. Hence, the yields of the solar thermal system are sufficient to fully charge the low-exergy storage. To illustrate this, data from February 4 to 9, 2020 was chosen as a representative operating period. Fig. 6a shows the solar irradiation (yellow) and the thermal power fed into each storage. The temperature limits for the control algorithm as well as the ambient temperature can be seen in the lower diagram (Fig. 6b).

Especially in the afternoon with comparably high ambient temperatures ranging between 0 and 10°C , the solar collectors provide high-temperature heat to the stratified storage. As soon as the top of the low-exergy storage detects a temperature of 20.2°C , the solar thermal energy is fed into the stratified storage. This storage is charged until the temperature at the top of the low-exergy storage drops below 15°C .

Considering all boundary conditions, the evaluation of the measurement data in Fig. 6 shows that the control algorithm meets the switching requirements. Moreover, the solar thermal system can fully charge the low-exergy storage with high effi-

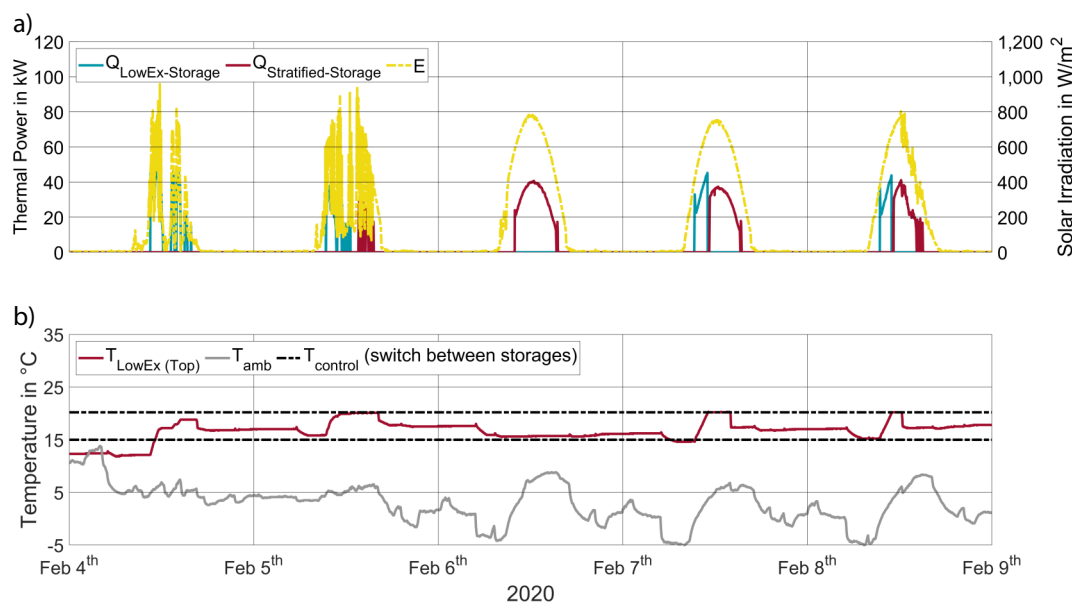


Figure 6. Representative measurement data from February 4 to 9, 2020: (a) Solar thermal power (in kW) and measured irradiation; (b) temperature at the top of the low-exergy storage (in $^\circ\text{C}$), ambient temperature (in $^\circ\text{C}$), and the operation range of the controller.

ciency even on winter days, due to lower operating temperatures.

In addition to the investigation of heat production for the storages, the behavior of the solar thermal collectors under real conditions η_{real} were evaluated and compared to the manufacturer's specifications. With the datasheet and real conditions of measured weather data, a theoretical efficiency $\eta_{\text{theoretical}}$ was determined according to Eqs. (1) and (2) [19]:¹⁾

$$\eta_{\text{Theoretical}} = \eta_0 - \frac{\alpha_1(T_m - T_{\text{amb}})}{E} - \frac{\alpha_2(T_m - T_{\text{amb}})^2}{E} \quad (1)$$

with:

$$T_m = \frac{(T_{\text{return}} + T_{\text{flow}})}{2} \quad (2)$$

For the calculations, the optical efficiency η_0 of 78.4 %, the linear heat loss coefficient α_1 ($4.142 \text{ W m}^{-2}\text{K}^{-1}$), the squared heat loss coefficients α_2 ($0.0038 \text{ W m}^{-2}\text{K}^{-2}$), and the collector aperture area A (89.6 m^2) from the manufacturer's datasheet are used. Considering the measured mean temperature of the heat transfer fluid T_m , the ambient temperature T_L , and solar irradiation E , a theoretical efficiency can be determined. These values were compared to the measured efficiency, i.e., the ratio between the heat delivered by the solar thermal collectors \dot{Q}_N and the incident irradiation (Eq. (3)) [19]:

$$\eta_{\text{Measurement}} = \frac{\dot{Q}_N}{E \times A} \quad (3)$$

To compare the measured with the theoretical efficiency, a winter day in February 2018 (Fig. 7) was chosen. The comparison indicates that the efficiency in case of real conditions is higher than the theoretical efficiency. Over the course of the day, the solar thermal collectors show an efficiency above 70 %. At the same time, the theoretical efficiency is determined at ~ 60 %. When evaluating the differences of the measured and expected efficiencies of the solar collectors according to the datasheet, the installation of the collector array has to be considered. As the solar thermal collectors are integrated into the roof of the central DHS, their heat losses are reduced, as the surrounding temperature is higher than the ambient temperature [20]. The higher efficiency of the solar thermal collectors can be observed through the whole year.

The high efficiency of the solar thermal collectors in combination with their ability to supply both the stratified or the low-exergy storage enables high solar thermal fractions at the Dollnstein system. Especially during summer, the lower heat demand of the customers in combination with a high collector yield allows for values greater than 60 % with respect to the overall heat production. In 2019, the solar thermal collector array delivered an overall amount of 69.8 MWh ($778 \text{ kWh m}^{-2}\text{a}^{-1}$) (Fig. 8), reflecting a total share of 6 % of the annual heat production.

3.3 High-Temperature Central Heat Pump

In the Dollnstein system, sector coupling should be enabled. Utilizing the central heat pump combined with the CHP is considered as a promising solution, demanding a more detailed investigation of the heat pump operation and efficiency. The central heat pump has a nominal thermal capacity of $440 \text{ kW}_{\text{th}}$ and is operated with the refrigerant, R744 (CO_2). It is a high-temperature heat pump with a maximal flow temperature of 80°C . Compared to conventional refrigerants, e.g. R134a, CO_2 has a critical temperature of 31.1°C [21]. Hence, to reach high flow temperatures, a CO_2 heat pump works in a transcritical area with high pressure ranging between 8 and 12 MPa [22].

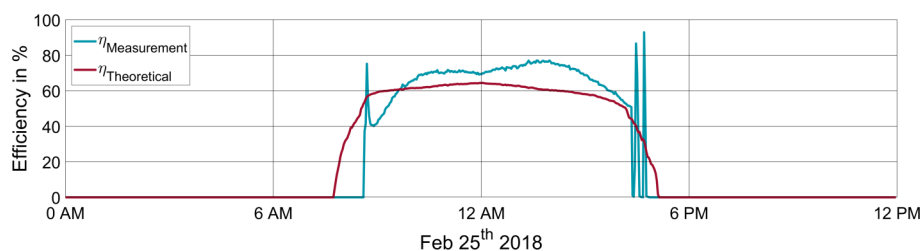


Figure 7. Comparison of the real and theoretical efficiencies of solar thermal collectors for a winter day.

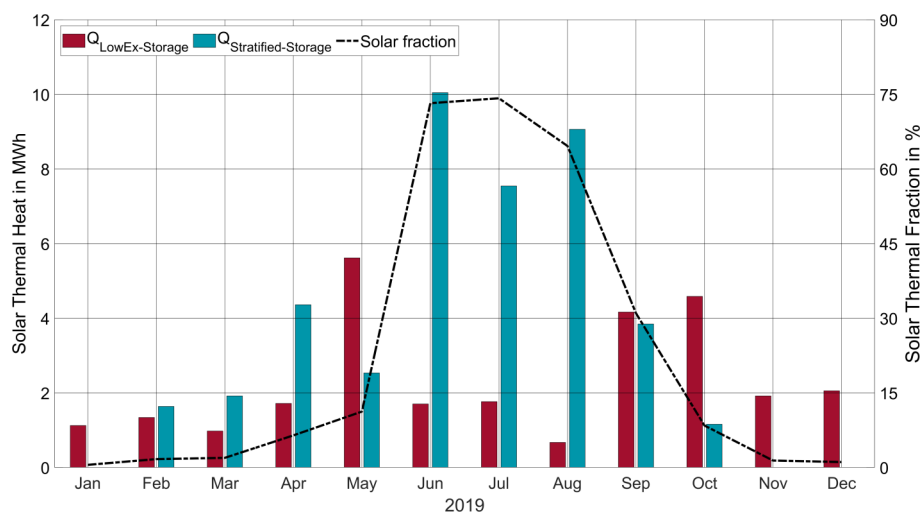


Figure 8. Solar thermal heat production in 2019.

1) List of symbols at the end of the paper.

This requires robust components to ensure safe operation. However, the use of CO₂ provides several advantages: It has a low global warming potential (GWP=1) and low flammability in case of malfunctions of the heat pump [21].

The central heat pump contains three compressors to generate a supply temperature of about 75 °C. To increase electricity self-consumption within the central district heating station the central heat pump is intended to run in parallel with the CHP plant and directly utilize the electricity produced. In 2019, the heat pump consumed 59.8 MWh of electrical energy, of which 16.4 % was taken from the external electricity grid. Especially during the winter months, the electric energy demanded from the external electricity grid decreased, which can be attributed to the simultaneous operation of both the central heat pump and the CHP plant. For instance, in December 2019, the electricity consumed from the external grid was only 3.27 % of the overall consumption of the heat pump.

Two groundwater wells and the low-exergy storage serve as heat sources for the heat pump. According to Fig. 1, the two wells charge the low-exergy storage with an annual mean temperature of 15 °C. Analyzing the heat meters reveals that 67 MWh of thermal energy is supplied by the two groundwater wells. However, the heat supply of the wells is limited by a precooling component upstream of the central heat pump (Fig. 9), which was originally not part of the system design but was necessary due to the sensitivity of the CO₂ heat pump.

The return of the DHN is cooled upstream of the central heat pump to lower the inlet temperature of the heat pump. As mentioned above, CO₂ heat pumps require a low inlet temperature at the condenser side to avoid a fault condition [23]. Thus, the temperature of the DHN return (Fig. 9; blue line) is decreased via a heat exchanger using the evaporator side circuit of the heat pump. In 2019, 60 MWh_{th} was transferred from the return side of the DHN to the well and may therefore be considered as heat loss.

Due to the very specific hydraulic setup of the heat pump in the Dollnstein system, there are two options to calculate its coefficient of performance (COP). First, a COP can be determined related to the heat pump itself. Temperatures after the precooling, directly at the in- and outlet of the heat pump, are

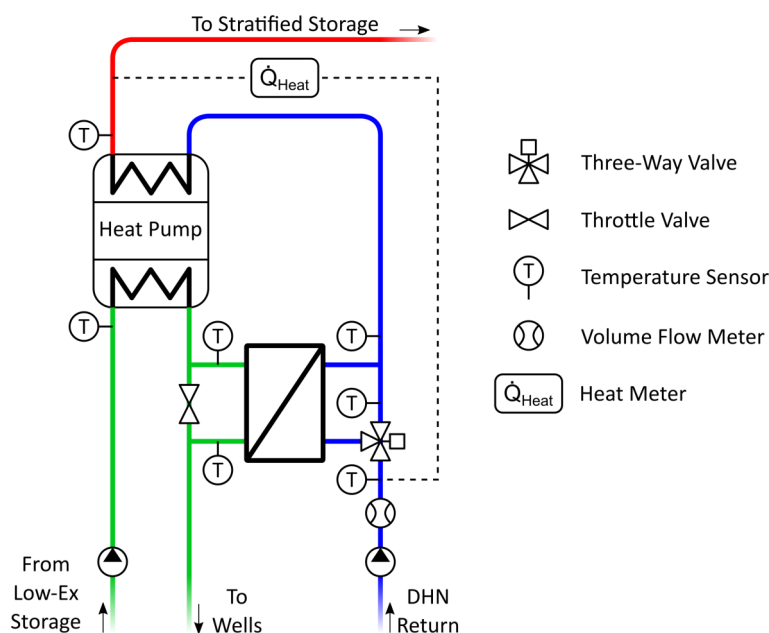


Figure 9. Precooling system of the central heat pump and measurement equipment.

used to derive this COP. Second, an effective COP with the precooling component can be determined. To check whether the heat pump works according to the manufacturer's datasheet, the COP of the heat pump itself was evaluated from the measurement data and compared to the manufacturer's information. To make those values comparable, specific operational points of the heat pump were considered. Only in case of the inlet and outlet temperatures being identical to the heat pump datasheet, the measured COP and the COP of the datasheet were compared.

Fig. 10 indicates that the seasonal temperature reduction has a significant impact on the efficiency of the heat pump. In 2019, the switch of the grid temperatures was on November 9. During the winter months, the heat pump works at an average COP of 2.4 (Fig. 10). Instead, due to a lower heating grid temperature and a higher temperature of the low-exergy storage, an average COP of 3.2 can be calculated during summer. Fig. 10 indicates that the calculated COP is close to the manufacturer's COP.

At some points, the compared COP values differ considerably. The reason for those peaks of the measured COP is that

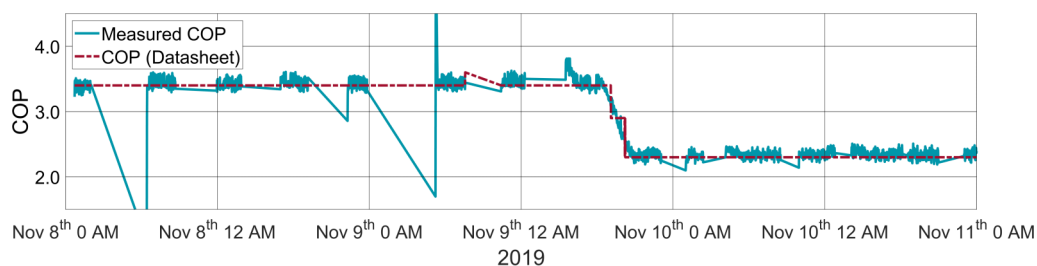


Figure 10. Comparison between the central heat pump COP according to the manufacturer's datasheet and the COP measured under real-life conditions between November 8 and 11, 2019.

the compressor of the heat pump turns off for a few minutes. Consequently, the flow rate of the heat sink approached $0 \text{ m}^3\text{h}^{-1}$. Comparing the COP, only the temperatures were taken into consideration. The volume flow rate was not considered, as it has a limited impact on the COP during the running process.

Evaluating the heat pump shows that the heat pump meets the manufacturer's specifications. However, the COP of the whole system is much lower due to the precooling component.

4 Discussion and Further Steps

This paper shows that seasonally lowering the flow temperature of a DHS reveals several optimization potentials for heat generation systems. As the heat demand of the consumers is lower than expected, annual heat losses could not be reduced compared to other DHN investigated by Pex [18]. However, it could be shown that lowering the supply temperatures in summer reduces the heat losses significantly. By utilizing both a low- as well as a high-temperature heat storage, the share of RE can be increased (in the present study, solar thermal fractions higher than 60 % were observed). To further increase the share of RE, the CHP plant should be fuelled with biomass instead of liquid gas, as it is the case in the current system.

Moreover, by connecting the operation of the CHP plant and the CO_2 heat pump, electricity self-consumption can be optimized (e.g., up to 83.6 % in 2019), especially in the winter months. Analyzing the measurement data shows that the whole system, especially the central heat pump, should be optimized, as the return temperature of the heating grid is higher than expected. Due to a non-ideal precooling component upstream of the CO_2 heat pump, heat is transferred to the well. Therefore, the groundwater wells cannot achieve their full potential as designed. Due to several technical problems with the existing CO_2 heat pump, it is planned to be replaced by a new one. Accordingly, the efficiency of the whole system is expected to improve, as the new heat pump is adapted to the current design of the DHN. To utilize further optimization potentials, a system model was developed within the research project using the Modelica programming language.

In conclusion, operating a DHN at different temperatures offers several advantages. As mentioned, e.g., by Ommen et al. [14] and Lund et al. [15], temperature-variable DHN have a high potential to increase the share of RE in the heating sector. Furthermore, the summer mode allows for integrating a higher share of RE especially in case of existing buildings with an increased heat demand. Utilizing decentral heat pumps enables coupling the electricity with the heating sector, which is considered as an advantageous feature of such DHN [9, 15]. However, the Dollnstein system requires further optimization measures, which will be further investigated by means of a simulation model. According to Yang and Svendsen [16], fourth-generation DHN are characterized by both a high energy efficiency and a high exergy efficiency (as compared to third-generation DHN). These advantages can be achieved by a seasonal temperature reduction and, thereby, reduced heat losses. However, such a setup is charged with higher investment costs and therefore requires further investigations.

Acknowledgments

The authors gratefully acknowledge the German Bundesministerium für Wirtschaft und Energie (BMWi) and the project management organization Projektträger Jülich (PtJ) for financially supporting the project NATAR ("Local heating grids with lowered temperature as provider of balancing power"; grant number: 03ET1425A). The authors furthermore thank all partners within the project for continuous support.

The authors have declared no conflict of interest.

Symbols used

A	$[\text{m}^2]$	collector aperture area
E	$[\text{W m}^{-2}]$	solar irradiation
P_{el}	$[\text{MWh}]$	electric energy delivered to the customers
$Q_{\text{Cons.}}$	$[\text{MWh}]$	heat consumed by the consumers
Q_{DHN}	$[\text{MWh}]$	heat delivered to the consumers from the central district heating station
Q_{loss}	$[\text{MWh}]$	heat losses
Q_{N}	$[\text{W}]$	available heat
$Q_{\text{LowEx-Storage}}$	$[\text{kW}]$	thermal power to low-exergy storage
$Q_{\text{Stratified-Storage}}$	$[\text{kW}]$	thermal power to stratified storage
T_{amb}	$[\text{°C}]$	ambient temperature
T_{control}	$[\text{°C}]$	limit temperature for the control algorithm
T_{flow}	$[\text{°C}]$	flow temperature
$T_{\text{LowEx(TOP)}}$	$[\text{°C}]$	temperature at the top of the low-exergy storage
T_{m}	$[\text{°C}]$	mean temperature of the heat transfer fluid
T_{return}	$[\text{°C}]$	return temperature

Greek symbols

α_1	$[\text{W m}^{-2}\text{K}^{-1}]$	linear heat loss coefficient
α_2	$[\text{W m}^{-2}\text{K}^{-1}]$	quadratic heat loss coefficient
η_0	$[-]$	optical efficiency
$\eta_{\text{Measurement}}$	$[-]$	efficiency under real-term working conditions
$\eta_{\text{Theoretical}}$	$[-]$	efficiency according to datasheet conditions

Abbreviations

CHP	combined heat and power
COP	coefficient of performance
DHN	district heating network
DHS	district heating station
EU	European Union
GWP	global warming potential
RE	renewable energy

SES

Smart Energy System

References

- [1] European Commission, *Communication from the Commission to the European Parliament, the European Council, the European Economic and Social Committee and the Committee of the Regions – The European Green Deal*, Brussels **2019**.
- [2] G. A. Marrero, *Energy Econ.* **2010**, 32, 1356–1363. DOI: <https://doi.org/10.1016/j.eneco.2010.09.007>
- [3] www.ec.europa.eu/eurostat/statistics-explained/index.php/Renewable_energy_statistics#Share_of_renewable_energy_almost_doubled_between_2004_and_2018 (accessed on February 09, 2021).
- [4] H. Lund, P. A. Østergaard, D. Connolly, B. V. Mathiesen, *Energy* **2017**, 137, 556–565. DOI: <https://doi.org/10.1016/j.energy.2017.05.123>
- [5] H. Lund, S. Werner, R. Wiltshire, S. Svendsen, J. E. Thorsen, F. Hvelplund, B. V. Mathiesen, *Energy* **2014**, 68, 1–11. DOI: <https://doi.org/10.1016/j.energy.2014.02.089>
- [6] H. Li, N. Nord, in *Proc. of the 16th Int. Symp. on District Heating and Cooling, DHC2018* (Ed: I. Weidlich), Energy Procedia, Hamburg **2018**.
- [7] H. Gadd, S. Werner, *Appl. Energy* **2014**, 136, 59–67. DOI: <https://doi.org/10.1016/j.apenergy.2014.09.022>
- [8] D. Schmidt, A. Kallert, M. Blesl, S. Svendsen, H. Li, N. Nord, K. Sipilä, in *Proc. of the 15th Int. Symp. on District Heating and Cooling* (Ed: R. Ulseth), Energy Procedia, Seoul **2016**.
- [9] S. Buffa, M. Cozzini, M. D'Antoni, M. Baratiari, R. Fedrizzi, *Renewable Sustainable Energy Rev.* **2019**, 104, 504–522. DOI: <https://doi.org/10.1016/j.rser.2018.12.059>
- [10] *Final Report of the IEA EBC Annex 64* (Eds: D. Schmidt, A. M. Kallert), Fraunhofer Institute for Energy Economics and Energy System Technology IEE, Stuttgart **2019**.
- [11] *Final Report of the IEA DHC Annex TS1* (Eds: D. Schmidt, A. M. Kallert), AGFW-Project Company, Frankfurt am Main **2017**.
- [12] N. Nord, E. K. L. Nielsen, H. Kauko, T. Tereshchenko, *Energy* **2018**, 151, 889–902. DOI: <https://doi.org/10.1016/j.energy.2018.03.094>
- [13] P. A. Østergaard, N. A. Andersen, *Energy* **2018**, 155, 921–929. DOI: <https://doi.org/10.1016/j.energy.2018.05.076>
- [14] T. Ommen, J. E. Thorsen, W. B. Markussen, B. Elmegaard, *Energy* **2017**, 137, 544–555. DOI: <https://doi.org/10.1016/j.energy.2017.05.165>
- [15] R. S. Lund, D. S. Østergaard, X. Yang, B. V. Mathiesen, *Int. J. Sustainable Energy Planning Manage.* **2017**, 12, 5–18. DOI: <https://doi.org/10.5278/ijsep.2017.12.2>
- [16] X. Yang, S. Svendsen, *Energy* **2018**, 159, 243–251. DOI: <https://doi.org/10.1016/j.energy.2018.06.068>
- [17] T. Ramm, M. Ehrenwirth, T. Schrag, in *Proc. of the 13th Int. Modelica Conf.* (Ed: A. Haumer), Linköping University Electronic Press, Regensburg **2019**.
- [18] B. Pex, Nahwärmenetze und Heizwerke – Erfolgsfaktoren und Erfahrungen, presented at *Conf. Wärme aus Biomasse – Stand der Technik und Perspektiven*, Straubing **2021**.
- [19] H. Watter, *Regenerative Energiesysteme*, vol. 5, Springer Vieweg, Wiesbaden **2019**.
- [20] T. Schabbach, P. Leibbrandt, *Solarthermie*, Springer Vieweg, Berlin, Heidelberg **2014**.
- [21] C. Aprea, A. Greco, A. Maiorino, *Int. J. Refrig.* **2013**, 36, 2148–2159. DOI: <https://doi.org/10.1016/j.ijrefrig.2013.06.012>
- [22] K. Nawaz, B. Shen, A. Elatar, V. Baxter, O. Abdelaziz, *Int. J. Refrig.* **2018**, 85, 213–228. DOI: <https://doi.org/10.1016/j.ijrefrig.2017.09.027>
- [23] P. Neksa, *Int. J. Refrig.* **2002**, 25, 421–427. DOI: [https://doi.org/10.1016/S0140-7007\(01\)00033-0](https://doi.org/10.1016/S0140-7007(01)00033-0)